

The plumbing of the global biological pump

Benoît Pasquier and Mark Holzer

School of Mathematics and Statistics, UNSW (b.pasquier@student.unsw.edu.au, mholzer@unsw.edu.au)

Introduction

The biological pump sets the state of the global ocean ecosystem and controls the atmosphere-ocean carbon balance with implications for climate change and ocean acidification. Nutrients are utilized by phytoplankton in the euphotic zone. Much of the resulting organic matter is transported into the aphotic zone as sinking particles. This biogenic transport *pumps* organic matter and carbon to depth where the organic matter is oxidized, regenerating the nutrient pool. Physical advective-eddy-diffusive transport makes nutrients available for utilization in the euphotic zone, completing the “plumbing of the biological pump”.

Here, following work from Holzer et al. [2013], we quantify the timescales and pathways that set the efficiency of the biological pump, where efficiency is quantified in terms of the proportion of carbon or nutrients sequestered at depth by the biological pump.

A simple phosphorous cycle

Because phosphate (PO_4) is necessary in the metabolism of all phytoplankton, we approximate PO_4 as the limiting nutrient here and link all biological production to the phosphate cycle. Denoting the concentration of PO_4 (Inorganic) and dissolved Organic phosphorus by P_I and P_O , we model the phosphate cycle as

$$\partial_t \begin{bmatrix} P_I \\ P_O \end{bmatrix} + \begin{bmatrix} \mathcal{T} + \gamma & -\kappa \\ 0 & \mathcal{T} + \kappa \end{bmatrix} \begin{bmatrix} P_I \\ P_O \end{bmatrix} = \begin{bmatrix} 0 \\ \mathcal{S}P_I \end{bmatrix} \quad (1)$$

where \mathcal{T} is the advective-eddy-diffusive transport operator, \mathcal{S} captures the biogenic particle transport (divergence of a Martin flux curve, where for every water column a fraction $(1-\sigma)$ of the uptake is assigned to the flux), and κ is the remineralization rate constant. For \mathcal{T} , we use the global steady-state data-assimilated operator of Primeau et al. [2013].

The biological pump

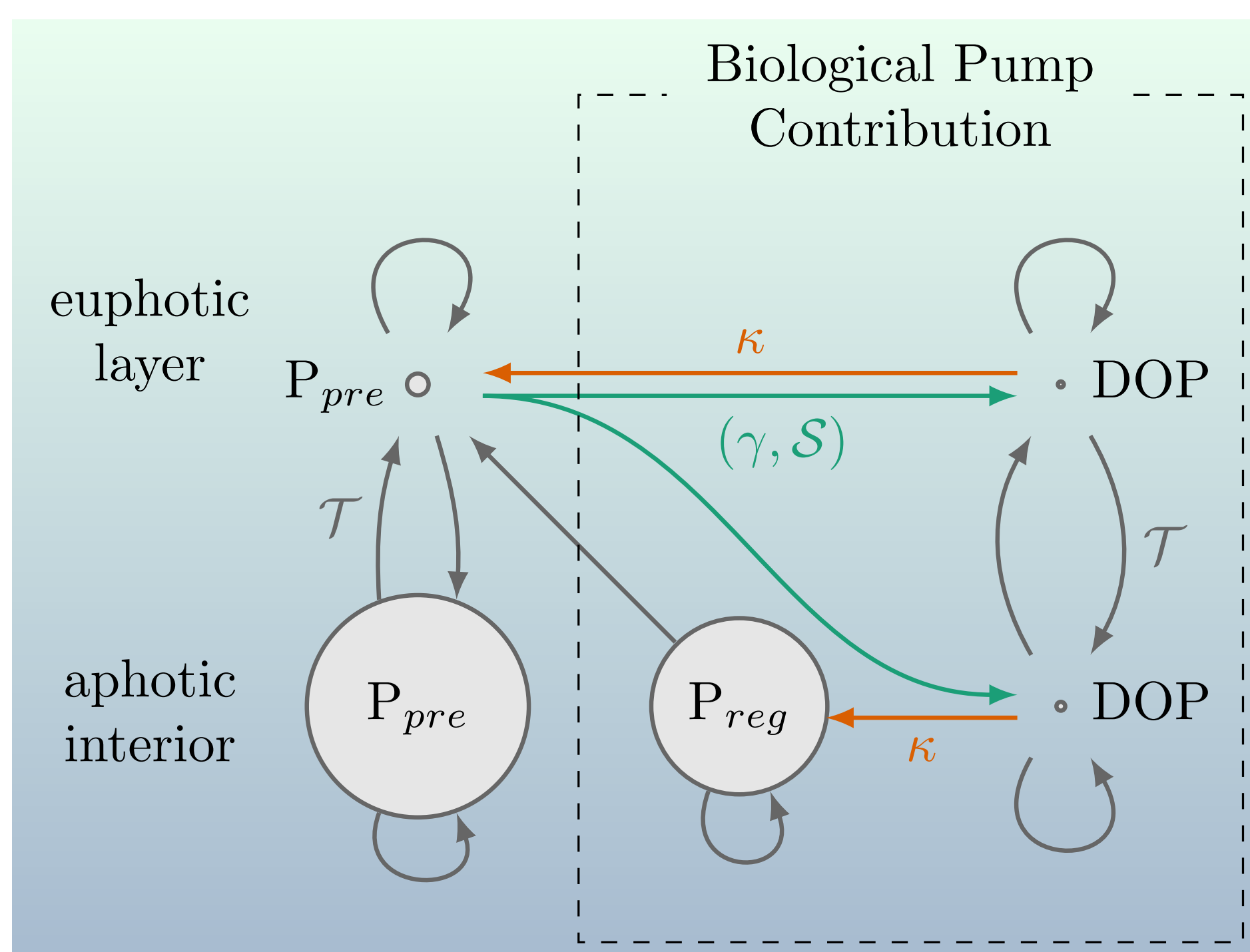


Fig. 1: Schematic of the transport and conversion rates between the preformed PO_4 , regenerated PO_4 , and DOP pools. Grey arrows represent advective-diffusive transport, green ones indicate uptake and biogenic transport, and orange ones represent remineralization.

Tracking phosphorus: Green functions

To track phosphorus from and to the euphotic zone, we use **forward** and **adjoint** Green functions:

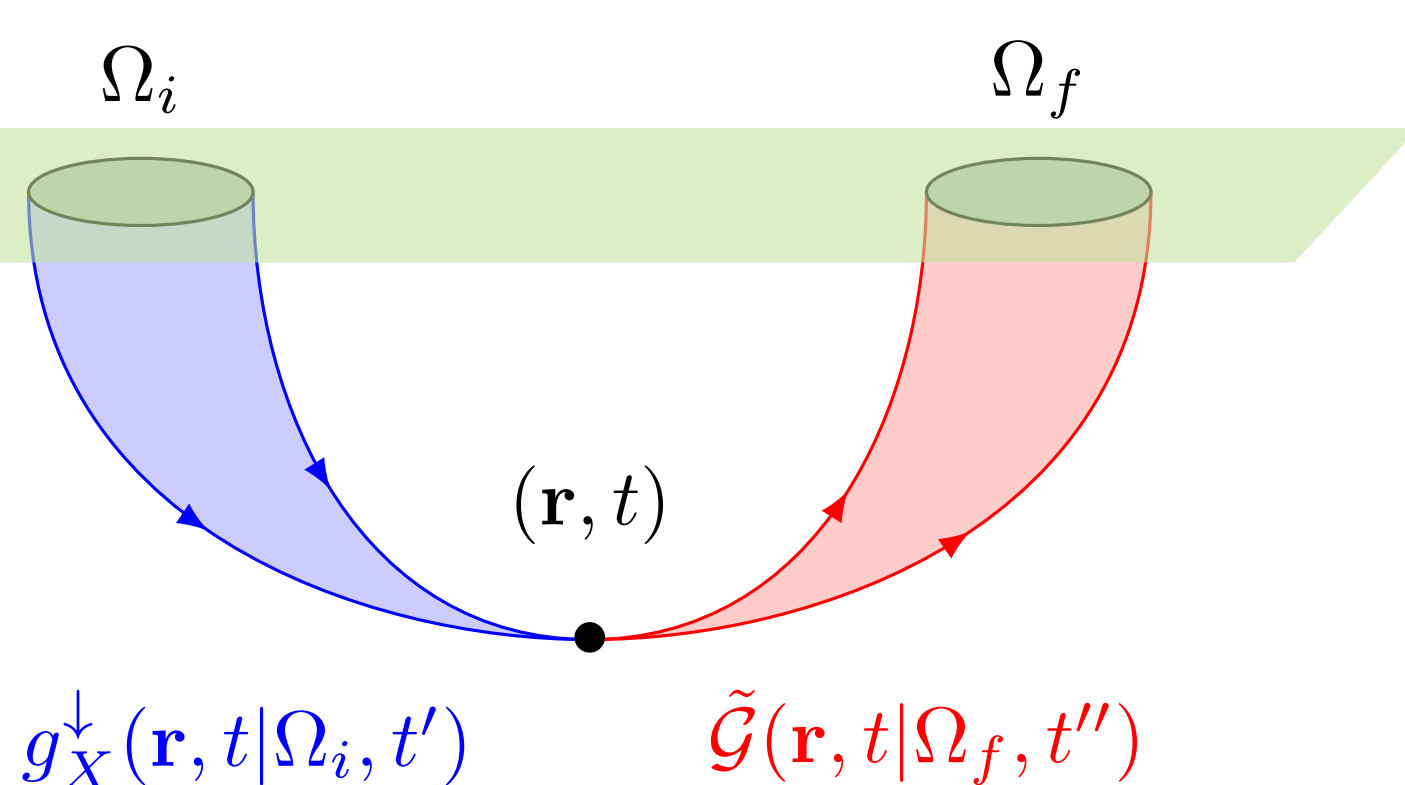


Fig. 2: Schematic of the forward and adjoint Green functions. The forward g_X^f is the contribution to the concentration at point (\mathbf{r}, t) that was last in euphotic region Ω_i at t' . The adjoint \tilde{G} represents the fraction of phosphorus at (\mathbf{r}, t) that is destined to reemerge in euphotic region Ω_f at t'' . For preformed PO_4 , $X=pre$ and for phosphorus that that has been biologically utilized (regenerated plus DOP), $X=bio$.

Euphotic regions (Ω_i and Ω_f)

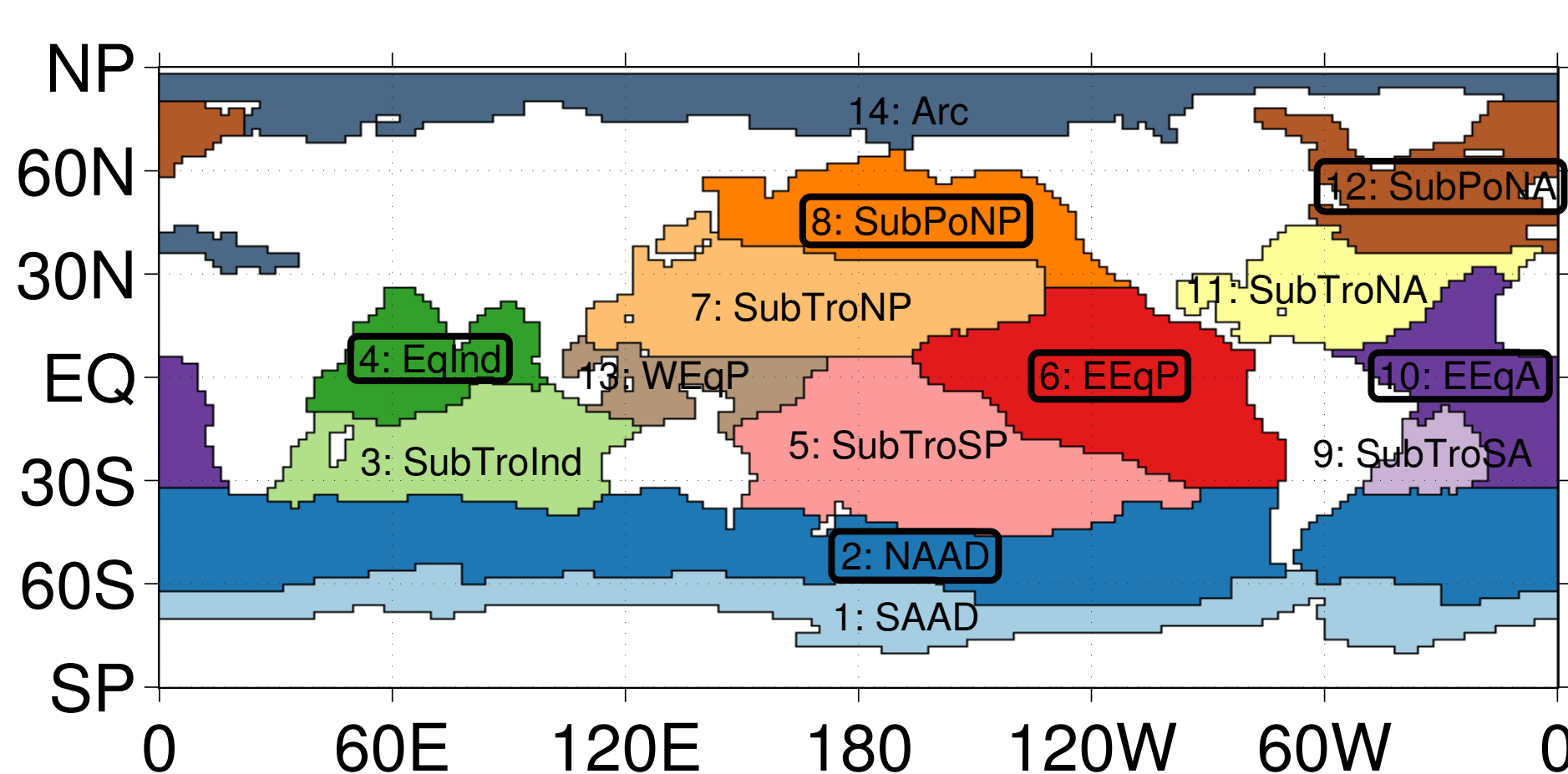


Fig. 3: Partition of the global euphotic zone (top 73.4) into regions Ω_i and Ω_f (initial and final) considered. The boundaries are based on productivity, except in the Southern Ocean, where SAAD and NAAD are separated by the location of maximum Ekman divergence. Regions of high production are highlighted. The color coding is used throughout.

Pump efficiency and leaks

The efficiency of the biological pump is defined as:

$$E_{bio} \equiv \frac{\mu_{bio}}{\mu_{tot}} = \frac{\mu_{tot} - \mu_{pre}}{\mu_{tot}} = 1 - L_{bio} \quad (2)$$

Here the μ 's are the global masses (total, preformed, or biologically utilized) in the ocean, which we can further partition according to where the phosphorus was last in the euphotic zone. With $X=bio$ or $X=pre$ these are obtained from the Green function as:

$$\mu_X(\Omega_i) = \int_{-\infty}^{\infty} dt \int d^3\mathbf{r} g_X^f(\mathbf{r}, t|\Omega_i) \quad (3)$$

The efficiency can be characterized as a consequence of its “leaks” (L_{bio}), which represent missed opportunities for phytoplankton to utilize the available nutrients in the euphotic zone. Here, we quantify where these leaks occur and how large they are:

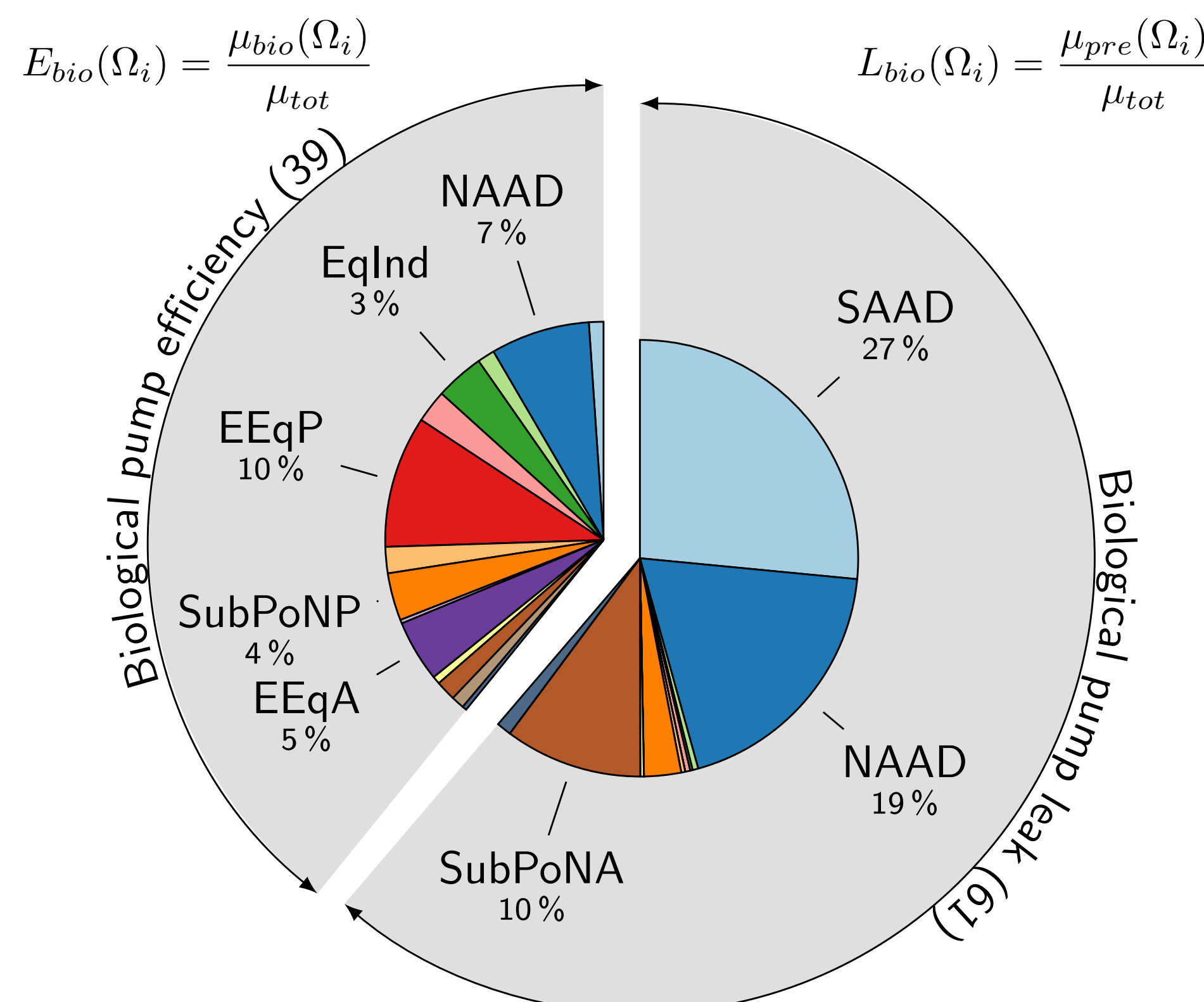


Fig. 4: Regional contributions to the pump’s efficiency and its leak.

Teleconnections (plumbing)

Using a fast relaxation in the euphotic zone (rate constant γ_a), we compute the flux into Ω_f of reemerging preformed and biologically utilized phosphorus of Ω_i origin, further partitioned according to the $\Omega_i \rightarrow \Omega_f$ transit time, t :

$$\mathcal{J}_X(t : \Omega_i \rightarrow \Omega_f) = \int d^3\mathbf{r} \Omega_f(\mathbf{r}) \gamma_a(\mathbf{r}) g_X^f(\mathbf{r}, t|\Omega_i). \quad (4)$$

Because of steady state, mass in transit in the $\Omega_i \rightarrow \Omega_f$ “pipe” that has transit time t is simply obtained from its flux flushing the pipe for a time t . Integrating over all transit times gives the mass in the $\Omega_i \rightarrow \Omega_f$ pipe.

$$\mu_X(\Omega_i \rightarrow \Omega_f) = \int_{-\infty}^{\infty} dt t \mathcal{J}_X(t : \Omega_i \rightarrow \Omega_f). \quad (5)$$

The fractional contributions of the $\Omega_i \rightarrow \Omega_f$ mass (of type $X=bio$) to the total mass (of type $X=bio$) in the ocean, reveals the biological teleconnections and quantifies their contributions to the global pump efficiency, E_{bio} . Note that $\mu_{bio} = \sum_{ij} \mu_{bio}(\Omega_i \rightarrow \Omega_f)$.

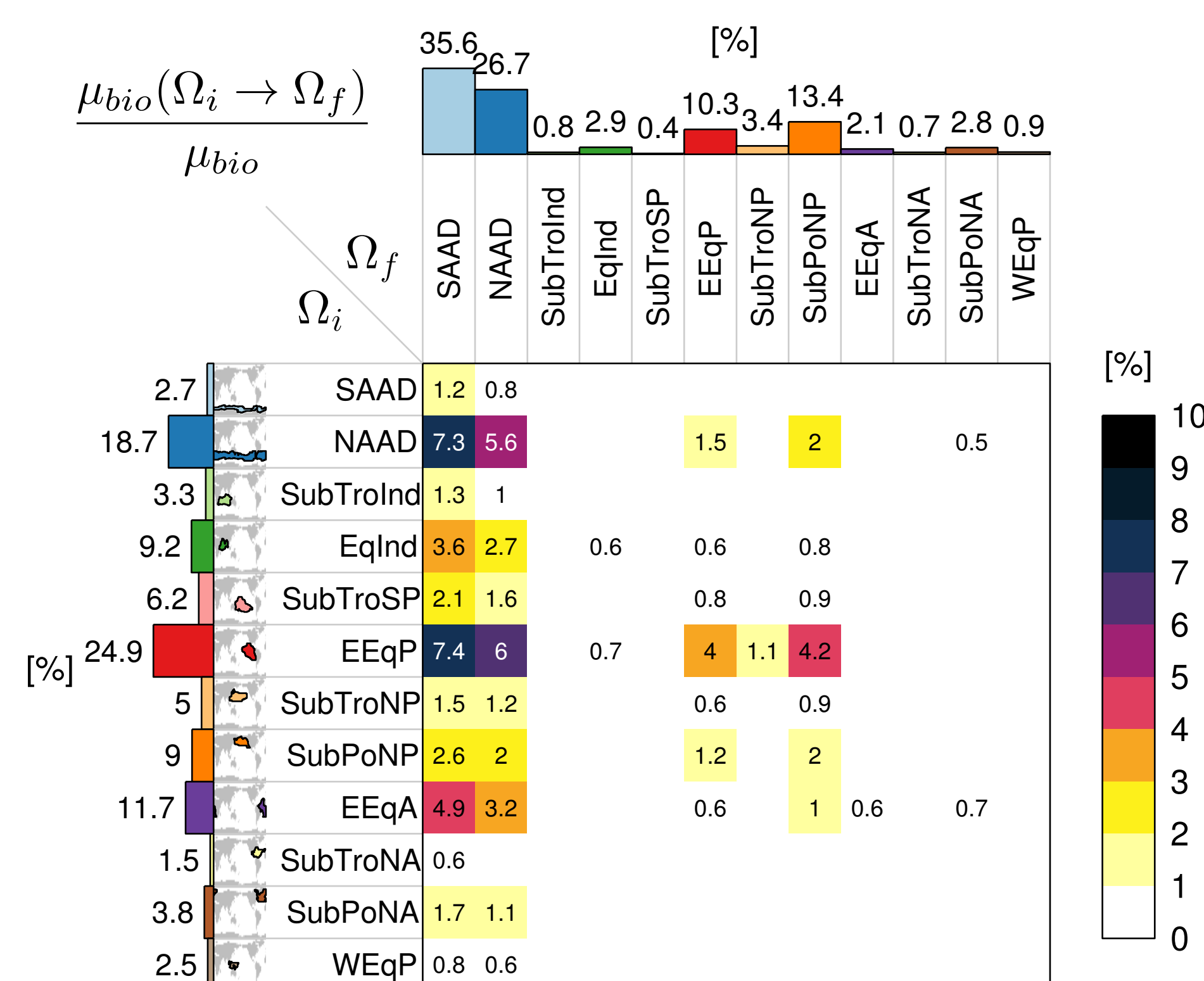
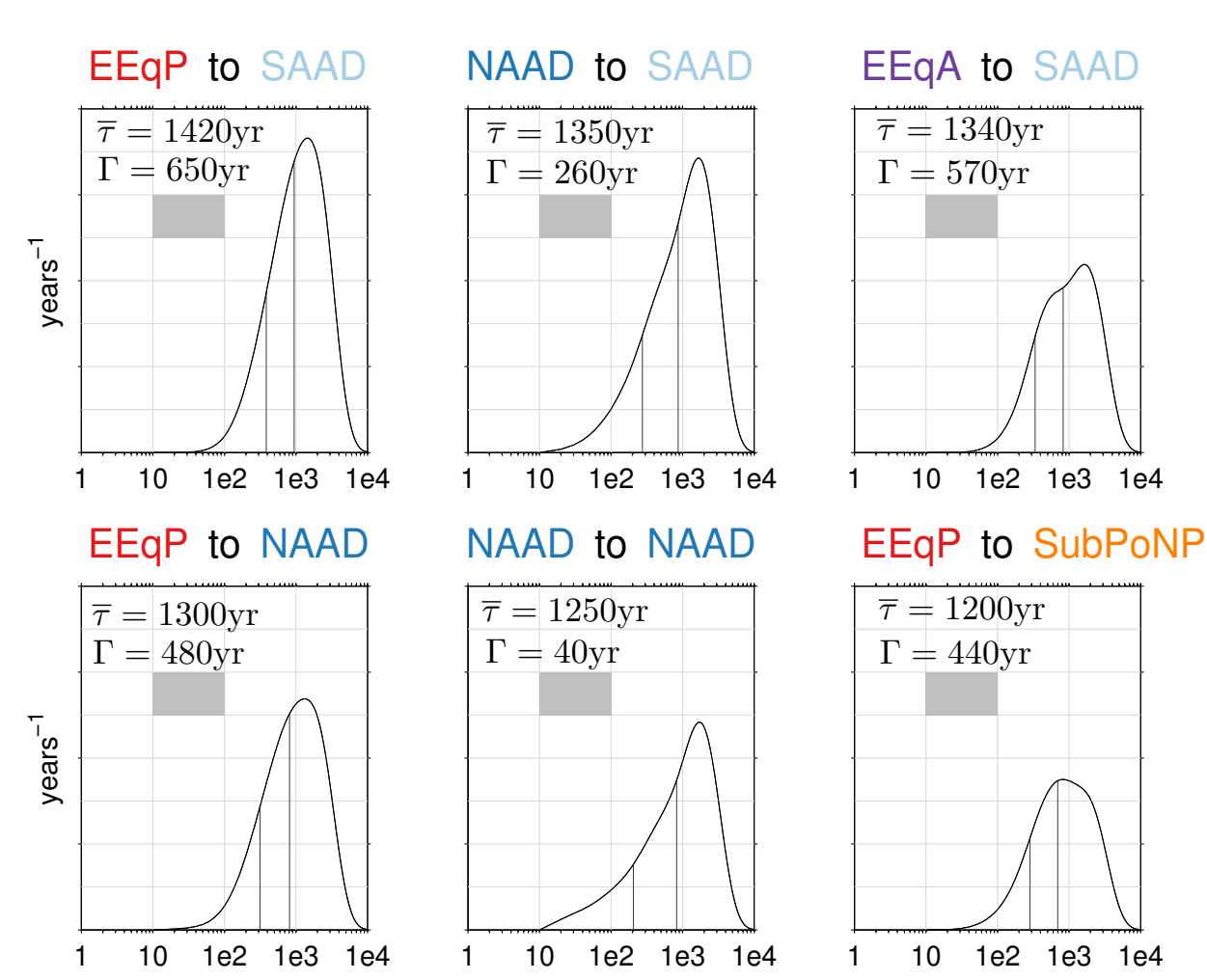


Fig. 5: Fractions (greater than 0.5%) of biologically utilized phosphorus in transit from Ω_i to Ω_f . The percentages in the margins represent the total contributions from Ω_i regardless of destination (left margin) and to the destinations to Ω_f regardless of origin (top margin).

$\Omega_f \rightarrow \Omega_f$ transit-time distributions

Fig. 6: Mass weighted, transit-time distributions (TTDs) of biologically utilized phosphorus for the six largest pipes of the pump. The grey rectangle represents a 1% contribution to E_{bio} . Vertical lines indicate the 1st and 3rd septiles of the TTD, convenient separations between fast, medium, and slow paths. The mean residence time $\bar{\tau}$ and the mean age on exit Γ are displayed for each $\Omega_i \rightarrow \Omega_f$ teleconnection.



Path densities

The density of phosphate molecules per unit volume at \mathbf{r} with a $\Omega_i \rightarrow \Omega_f$ transit time τ can be obtained schematically as:

$$d\tau \eta_{bio}(\mathbf{r}, \tau|\Omega_i \rightarrow \Omega_f) = d\tau \int_0^\tau dt \tilde{G}(\mathbf{r}, \tau - t|\Omega_f) g_{bio}^f(\mathbf{r}, t|\Omega_i). \quad (6)$$

Note that this is also the density of the paths of phosphate molecules last utilized in Ω_i destined for reemergence on Ω_f .

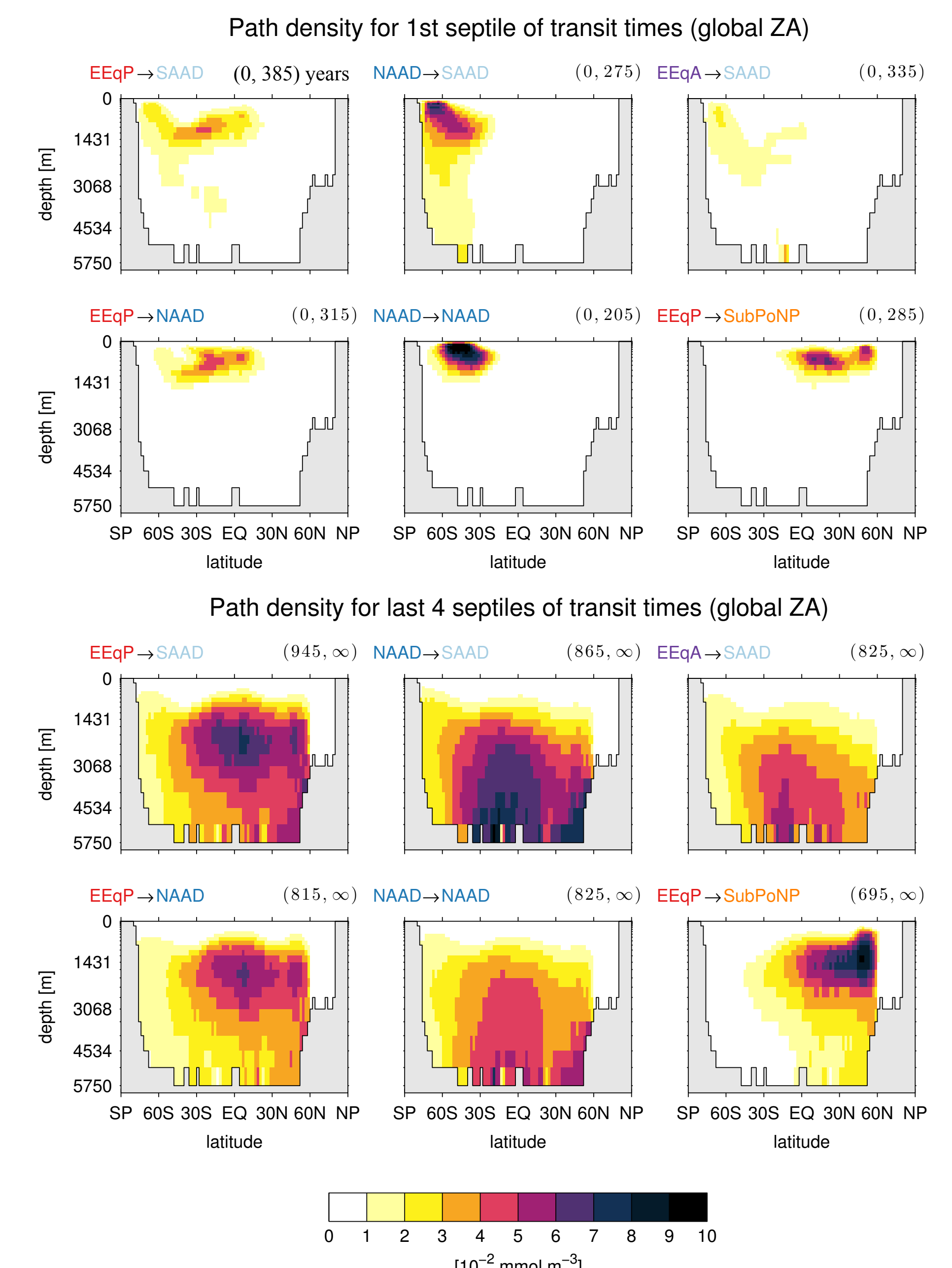


Fig. 7: Top Panel: Global zonal averages of the $\Omega_i \rightarrow \Omega_f$ path density of fast paths for the 6 largest $\Omega_i \rightarrow \Omega_f$ “pipes” of the biological pump. Time-band integrated over is indicated at the top right corner of each plot [years]. Bottom Panel: same for slow paths.

Uncertainty estimation

The robustness of the results has been assessed by computing all quantities over an ensemble of 10 data-assimilated circulations with slightly different objective functions [DeVries, 2014]. In general values vary by ± 5 -10% across the ensemble.

Conclusions

- The biologically utilized phosphorus (regenerated PO_4 plus DOP) that sets an efficiency of $E_{bio} = (39 \pm 2)\%$ is dominated by contributions from highly productive regions: the Eastern Equatorial Pacific (EEQP) and Atlantic (EEQA), the Equatorial Indian Ocean (EqInd), the Subpolar North Pacific (SubPoNP), and the Southern Ocean North of the Antarctic Divide (NAAD). These five regions account for $(74 \pm 1)\%$ of E_{bio} .
- The high-latitude regions, (Southern Ocean, Subpolar North Atlantic and Pacific), account for $(96 \pm 1)\%$ of the pump leak. Unlike for the efficiency, for which NAAD dominates, both the regions south and north of the Antarctic divide (SAAD and NAAD) make comparable contributions totalling $(75 \pm 3)\%$ of the leak.
- $(51 \pm 1)\%$ of the biological pump efficiency is teleconnected through merely eleven $\Omega_i \rightarrow \Omega_f$ pipes out of a total of $14 \times 14 = 196$ possible (Ω_i, Ω_f) pairs.
- The six teleconnections making the greatest contributions to the biological pump are EEQP \rightarrow (SAAD, NAAD), NAAD \rightarrow (SAAD, NAAD), EEQA \rightarrow SAAD, EEQP \rightarrow SubPoNP. These connect regions of high production to regions of high upwelling via slow, deep, eddy-diffusive paths.
- The Southern Ocean is where $(67 \pm 5)\%$ of the phosphorus mass in the ocean reemerges into the euphotic zone as bioavailable phosphate.
- The mean age on exit of the phosphate reemerging in the Southern Ocean is $\Gamma = 200 \pm 5$ years since it was last biologically utilized, for a mean residence time $\bar{\tau} = 1400 \pm 20$ years (Note that the mean age on exit Γ is generally much shorter than the mean residence time $\bar{\tau}$ in the ocean interior for advective-diffusive flow, see Fig. 6).
- The $\Omega_i \rightarrow \Omega_f$ “pipes” that contribute most to the pump efficiency have transit-time distributions for which the paths in the first septile are faster than 200-300 years. 4/7 of the mass of regenerated PO_4 and DOP in these pipes have transit times longer than 700-900 years.
- The bulk of the pump efficiency is carried by slow paths that sequester a large mass μ_{bio} in the deep ocean below the thermocline. These slow paths are highly eddy-diffusive and distribute the mass in $\Omega_i \rightarrow \Omega_f$ transit throughout the world oceans.

Acknowledgement: This work was supported by grant DP120100674 from the Australian Research Council (MH).

References

- Holzer, M., and F. Primeau, Global teleconnections in the oceanic phosphorus cycle: patterns, paths, and timescales. *J. Geophys. Research*, 118, 1775-1796, doi:10.1002/jgrc.20072, 2013.
- Primeau, F., M. Holzer, and T. DeVries, Southern Ocean nutrient trapping and the efficiency of the biological pump. *J. Geophys. Research*, 118, 2547-2564, doi:10.1002/jgrc.20181, 2013.
- DeVries, T., The oceanic anthropogenic CO_2 sink: Storage, air-sea fluxes, and transport over the industrial era. *Global Biogeochem. Cycles*, 28, 631-647, doi:10.1002/2013GB004739, 2014.